



Benzotriazole as inhibitor for copper with and without corrosion products in aqueous polyethylene glycol

E. GUILMINOT*¹, J.-J. RAMEAU¹, F. DALARD¹, C. DEGRIGNY² and X. HIRON³

¹Laboratoire d'Electrochimie et de Physico-chimie des Matériaux et des Interfaces, 1130 Rue de la Piscine, Domaine Universitaire, BP 75, 38402 Saint Martin d'Hères, France;

²Laboratoire Arc'Antique, 26 Rue de la Haute Forêt, 44300 Nantes, France;

³Laboratoire ARC-Nucléart, C.E.N.G., 17 Rue des Martyrs, 38054 Grenoble, France

(* Author to whom correspondence should be addressed)

Received 5 March 1998; accepted in revised form 22 September 1998

Key words: benzotriazole, corrosion, copper, inhibitor, polyethylene glycol (PEG)

Abstract

Electrochemical methods, including polarization experiments and impedance spectroscopy, were used to evaluate the effectiveness of benzotriazole (BTA) in an aqueous solution of polyethylene glycol (PEG) in protecting polished archaeological copper or archaeological copper covered with corrosion products. The adsorption of PEG on the polished copper significantly limited the corrosion current. The presence of benzotriazole enhanced the protection of the polished copper, giving maximum protection at a concentration of $10^{-2} \text{ mol l}^{-1}$ of BTA in 20 vol % PEG 400 solution. On the other hand, PEG solutions caused degradation of the corrosion products of the copper. This degradation increased with time. When BTA was added, the corrosion products were preserved and, the higher the BTA concentration, the more the corrosion current decreased. In PEG 400 solution protection of the corrosion products of the copper by BTA improved over time.

1. Introduction

Many archaeological objects made of wood have composite copper parts which cannot be separated from the wood. If they are to be conserved in the long term they have to be treated. Such treatment generally focuses on the most fragile of the materials, namely the waterlogged wood. This generally involves impregnating the object with polyethylene glycol (PEG) followed by freeze drying or controlled air drying [1].

In its atmospheric corrosive environment, copper becomes covered with stable corrosion products which form a pseudo-protective layer, commonly called 'patina' [2]. This patina must be preserved for aesthetic reasons. During the phase when the wood is impregnated, certain metal parts are usually protected through the addition of a corrosion inhibitor. In the case of ferrous metals, products such as Hostacor[®] are currently undergoing tests [3, 4]. For cuprous metals, tests have been performed by replacing PEG with Witcamine[®] RAD1100 [3], a polymer which has inhibiting properties with respect to copper corrosion, but this product is not as effective as PEG for consolidating wood. To protect the copper and its patina during impregnation of the wood, it is preferable to use PEG and add a copper corrosion inhibitor. A product which has been reported in the literature to be effective in other acid and neutral

conditions, the benzotriazole (BTA), has been studied here [5, 6].

The aim of the study was to check the effectiveness of this inhibitor in an H₂O–PEG solution for polished archaeological copper and for archaeological copper covered with corrosion products. Electrochemical methods such as anodic and cathodic polarization and impedance spectroscopy were used.

2. Experimental conditions

2.1. Archaeological copper

The copper samples came from a rivet from the wooden structure of a ship that had been wrecked to the west of Lorient at the beginning of the 19th century. The samples were removed in 1995 and kept in tap water which was regularly renewed.

Analysis of the elements showed that the metal was 99% copper. Numerous inclusions, containing nickel, lead, arsenic and antimony, were distributed inside the grains. The corrosion products formed a very fissured, complex layer, varying in thickness from 2 to 10 μm . A layer of cuprite, Cu₂O, and chlorides was in contact with the copper and carbonates were present at the external interface.

2.2. Electrolytes

The solutions were composed of PEG 400 (20 vol %) in deionized water. This is a solution used to thoroughly impregnate waterlogged wood. To reproduce as closely as possible the treatment conditions for archaeological wood, the electrolytes were thermostatically controlled at 25 °C and were not deaerated; the pH was 5.9 and the addition of benzotriazole at a concentration varying from 10^{-5} to $8 \times 10^{-2} \text{ mol l}^{-1}$ modified the pH very little (~ 5.8); acidic or basic conditions degrade the wood.

2.3. Determination of electrochemical characteristics

The electrochemical characteristics were determined using a double-walled, three-electrode Metrohm cell placed in a Faraday cage. The reference electrode used was a calomel electrode in a saturated solution of KCl ($E_{\text{SCE}} = 0.245 \text{ V}$ vs standard hydrogen electrode SHE). Contact with the solution was made via a tube filled with KNO_3 at $10^{-2} \text{ mol l}^{-1}$. The counter electrode was a platinum grid. The working electrode, made of archaeological copper, was fitted to a Radiometer EDI 101T revolving electrode cap with the speed maintained constant at 500 rpm. The surface was polished using sandpaper up to 4000 grit then with felt and a diamond-charged suspension ($3 \mu\text{m}$ size). The measurements performed on the copper with corrosion products were performed without stirring. The effective surface area was 0.25 cm^2 , delimited by varnish (Paraloid B72 diluted at 60% in ethanol).

Cyclic voltametry was carried out using a Radiometer PGP 201 digital potentiostat, controlled by Voltalab 21 software. Data were plotted at a scan rate of 1 mV s^{-1} after a 4 h wait at the corrosion potential (or 10 h for copper covered with corrosion products). For the impedance spectroscopy the set-up included a Schlumberger/Solartron 1287 electrochemical interface, and a 1250 frequency response analyser, controlled by Zplot-

Zview software applications. Following stabilization of the potential, impedance measurements were carried out at the corrosion potential in the frequency range from 50 kHz to 10 mHz (or 1 mHz) with a sinusoidal disturbance amplitude of 50 mV.

3. Experimental results

3.1. Polished copper

The corrosion potential before polarization is more anodic in the presence of BTA. Benzotriazole is reported to have a greater effect on the anodic dissolution of copper than on the cathodic reduction of dissolved oxygen [7]. The polarization curve of the polished copper in a nondeaerated solution of PEG 400 at 20% has an anodic plateau and a cathodic region where the absolute value of the current density is less than $10 \mu\text{A cm}^{-2}$ (Figure 1). The current density in the cathodic region depends on the PEG 400 concentration. At -600 mV vs SCE it was $-2.5 \mu\text{A cm}^{-2}$ for 0.2% PEG 400 (Figure 1) and it dropped by a factor of 8 when the PEG concentration reached 20%. The higher the PEG concentration the greater the decrease in the absolute value of the current density. This is due to adsorption of PEG on the copper surface [8].

The impedance spectroscopy diagrams obtained for polished copper in H_2O -PEG solution (irrespective of the benzotriazole concentration), at the corrosion potential, were identical when the line was plotted at rising or falling frequencies, or when the sinusoidal disturbance amplitude (ΔE) was changed (Figure 2). The system may, therefore, be considered linear and steady state. The impedance spectrum of the copper in 20% PEG 400 solution comprised a single capacitive loop. This is generally equivalent to an electric circuit comprising the resistance of the electrolyte R_e ($\sim 5 \text{ k}\Omega$ in our case), in series with the double-layer capacitance C_{dl} in

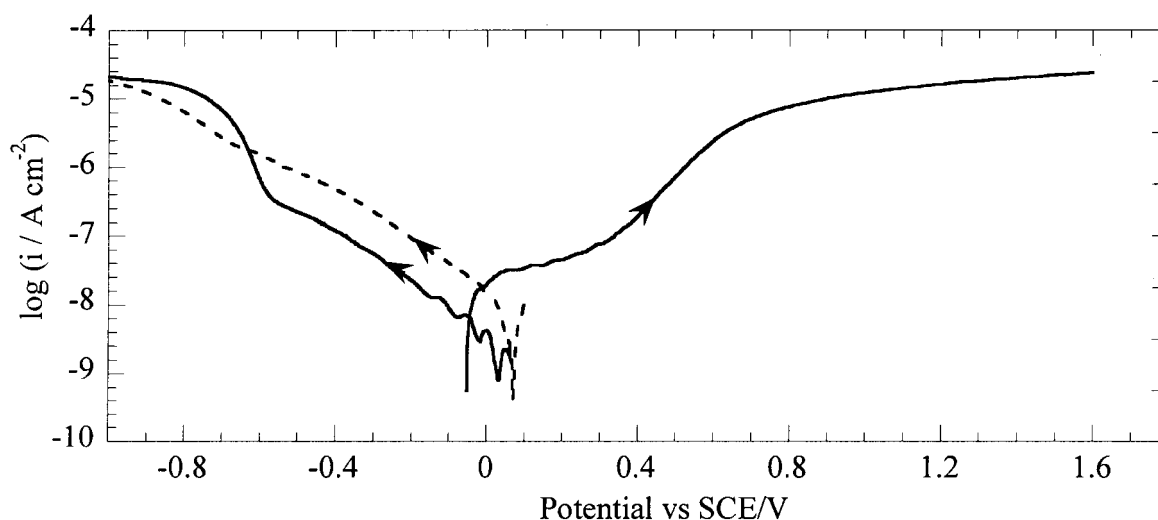


Fig. 1. Polarization curves of polished archaeological copper at 25 °C and 1 mV s^{-1} in aqueous solutions of 20% PEG 400 (—) and 0.2% PEG 400 (- - -).

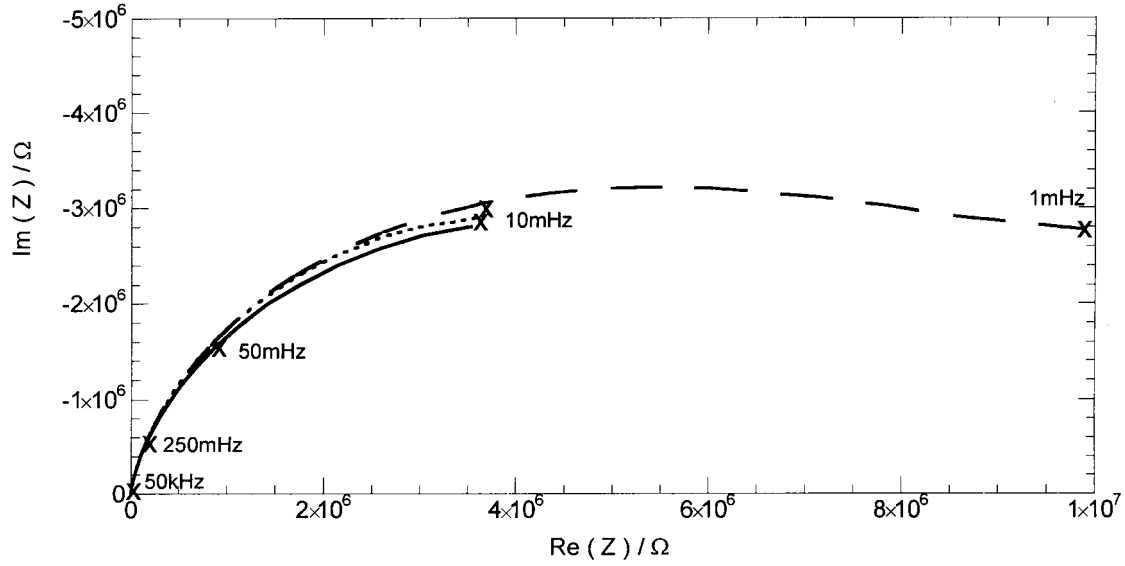


Fig. 2. Nyquist diagram showing impedance spectrum for polished copper, at the corrosion potential, in an aqueous solution of 20% PEG 400 with $10^{-2} \text{ mol l}^{-1}$ of BTA, 25°C , with sweep widths of (—) 50 KHz to 10 mHz, of (- - -) 10 mHz to 50 kHz, and of (- · -) 50 kHz to 1 mHz.

parallel with a polarization resistance R_p . When the semicircle has a large dephasing, the simulation has no physical significance [9]. It is thought the formation of the adsorbing polymer (PEG) creates a new capacitive loop at low frequencies [8–12]. The circuit was modified by introducing an adsorption resistance R_{ad} in parallel with an adsorption capacitance C_{ad} (Figure 3) [9, 11, 12]. A numerical simulation of this circuit for the H_2O –PEG–copper interface was performed and the experimental curve was fitted in order to determine the values of the different constituents (Table 1): the double layer capacitance C_{dl} is of the order of $1.4 \mu\text{F cm}^{-2}$, the polarization resistance, R_p , is approximately $3 \text{ k}\Omega \text{ cm}^2$, the resistance R_{ad} is $2 \text{ M}\Omega \text{ cm}^2$ and the adsorption capacitance of $1.2 \mu\text{F cm}^{-2}$ is associated with a phase angle α of 0.7 corresponding to the surface roughness of the copper [9]. To validate this circuit, the impedance of the system was measured at an anodic potential of $+150 \text{ mV}$ vs SCE. The capacitive loop of the double layer should not modify [9], but the capacitive loop of the PEGs adsorption becomes an inductive loop [9, 13].

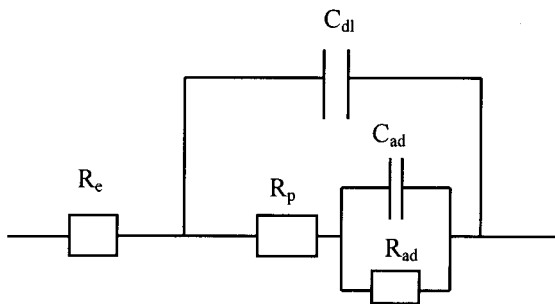


Fig. 3. Model of electric circuit simulating the system of copper in 20% PEG 400 solution at corrosion potential. Key: (R_e) electrolyte resistance; (C_{dl}) double layer capacitance; (R_p) polarization resistance; (C_{ad}) adsorption capacitance; (R_{ad}) adsorption resistance.

The spectrum was in the form of a capacitive, then an inductive arc (Figure 4). The part of the diagram between 50 and 5 kHz can be explained by the geometry of the cell. The separation of the two arcs made it possible to determine more precisely the values of C_{dl} and R_p . The spectrum simulation in Figure 4 gives a double-layer capacitance of $1.4 \mu\text{F cm}^{-2}$ and a polarization resistance of $3.5 \text{ k}\Omega \text{ cm}^2$. These values are of the same order of magnitude as those determined at the corrosion potential.

This study of the impedance spectra of the polished copper in H_2O –PEG solution shows that PEG was adsorbed on the copper surface. The fact that this

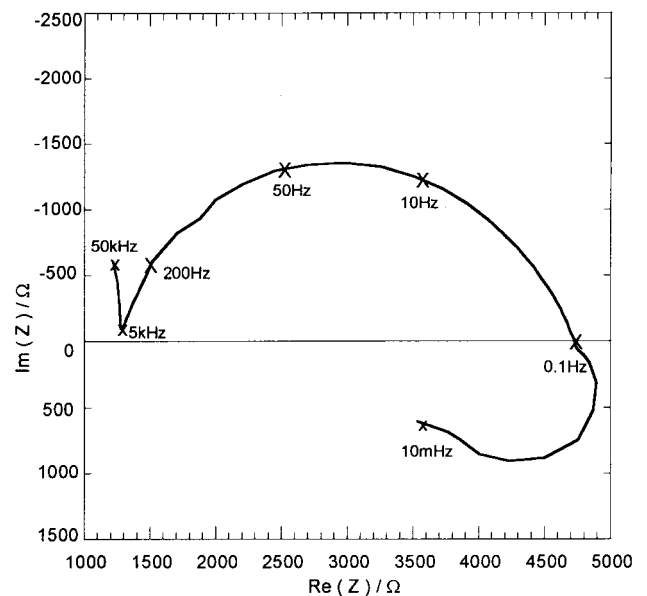


Fig. 4. Nyquist diagram showing impedance spectrum for polished copper, at $+150 \text{ mV}$ vs SCE in an aqueous solution of 20% PEG 400 at 25°C .

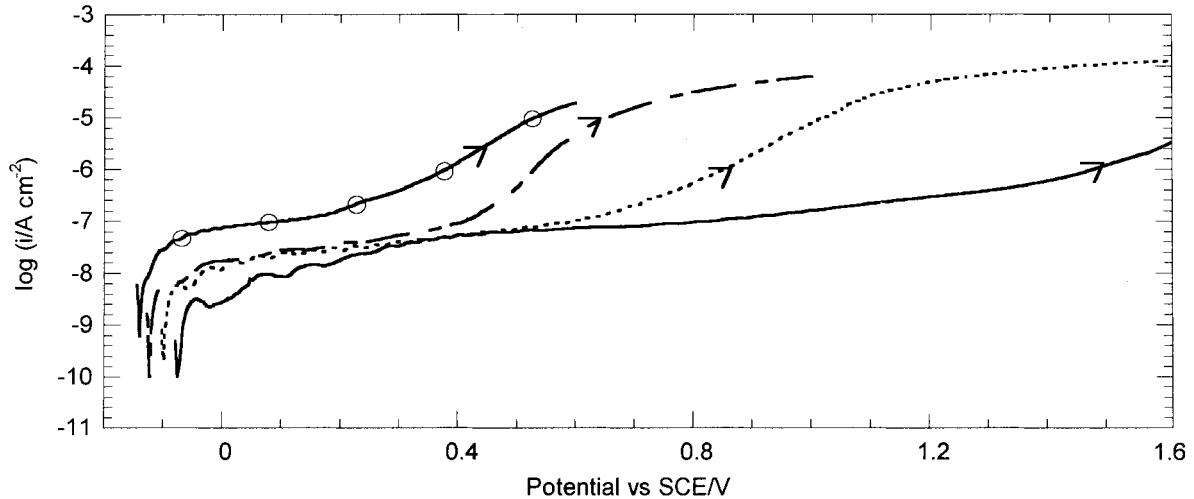


Fig. 5. Anodic polarization curves of polished archaeological copper, at 25 °C and 1 mV s⁻¹, in aqueous 20% PEG 400 solutions with BTA. Amount of BTA: (—) 8×10^{-2} , (- - -) 10^{-3} , (- · -) 10^{-4} and (· · ·) 10^{-5} mol l⁻¹.

adsorption limits the number of active sites confirms the low corrosion determined on the polarization curves (Figure 1).

When benzotriazole was added a low anodic current density was obtained confirming the predominantly anodic character of the BTA action mechanism on the copper. The extent of this anodic plateau increased with benzotriazole concentration (Figure 5).

The impedance spectra plotted at the corrosion potential in the presence of benzotriazole (Figure 6) are identical in shape to that obtained without BTA. They can thus be characterized by the same equivalent electrical circuit described in Figure 3. The action mechanism of BTA on the copper includes an adsorption phase [6], so there is a risk of competitive adsorption between the BTA and the PEG on the surface. The spectra simulation in Figure 6 shows that

the values of C_{dl} were less than $1 \mu\text{F cm}^{-2}$, irrespective of the benzotriazole concentration (Table 1). The polarization resistance, R_p , was approximately $6 \text{ k}\Omega \text{ cm}^2$ for 10^{-5} M of BTA and reached a maximum of $10 \text{ k}\Omega \text{ cm}^2$ for a BTA concentration of 10^{-3} mol l⁻¹. The increase in polarization resistance and the decrease in capacitance C_{dl} in the presence of BTA corresponds to a drop in the dissolution current [14]. The variations in the capacitive loop of adsorption are more significant. The values of R_{ad} (Table 1) increased in the presence of BTA, reaching a maximum for a concentration of around 10^{-2} M. The BTA therefore reduced the number of active sites on the copper and produced a more protective film than the PEG. The effectiveness of BTA on the polished copper in H₂O-PEG was optimal for a concentration of around 10^{-2} mol l⁻¹ (for a ratio (area of Cu)/(volume of solution) of $2 \text{ cm}^2 \text{ l}^{-1}$).

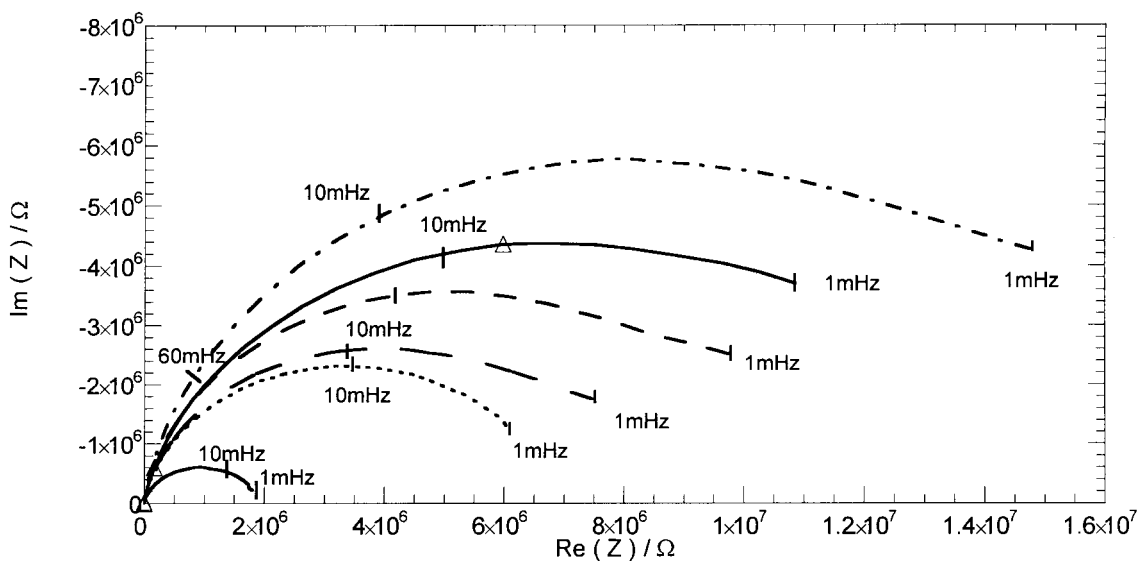


Fig. 6. Nyquist diagram showing impedance spectrum for polished copper, at corrosion potential, at 25 °C, in an aqueous solution 20% PEG 400 with BTA. Amount of BTA: (—) 0, (- - -) 10^{-4} , (- · -) 10^{-2} , (· · ·) 10^{-5} , (- - -) 10^{-3} and (-Δ-) 8×10^{-2} mol l⁻².

Table 1. Summary of impedance spectroscopy results for polished copper and copper covered with corrosion products

20% PEG 400 solution with:	Polished copper				Copper covered with corrosion products			
	C_{dl} / $\mu\text{F cm}^{-2}$	R_p / $\text{k}\Omega \text{cm}^2$	C_{ad} / $\mu\text{F cm}^{-2}$	R_{ad} / $\text{M}\Omega \text{cm}^2$	C_{dl} / nF cm^{-2}	R_p / $\text{k}\Omega \text{cm}^2$	C_{ad} / $\mu\text{F cm}^{-2}$	R_{ad} / $\text{k}\Omega \text{cm}^2$
0% of BTA	1.4	3	1.2	2	75	0.3	15	18
10^{-5} mol l^{-1} of BTA	0.7	6	$\alpha = 0.7$ 0.4	7	10	1.6	$\alpha = 0.50$ 2.5	60
10^{-4} mol l^{-1} of BTA	0.8	7	$\alpha = 0.65$ 0.5	8	20	1.2	$\alpha = 0.45$ 4.5	50
10^{-3} mol l^{-1} of BTA	0.8	10	$\alpha = 0.6$ 0.6	11	15	1.5	$\alpha = 0.55$ 2	100
10^{-2} mol l^{-1} of BTA	0.7	8	$\alpha = 0.7$ 0.6	16	30	2.4	$\alpha = 0.65$ 3	250
8×10^{-2} mol l^{-1} of BTA	0.6	5	$\alpha = 0.6$ 0.1	13	10	4	$\alpha = 0.6$ 2	500

3.2. Copper covered with corrosion products

The cathodic polarization curve of the copper covered with corrosion products in 20% PEG 400 solution (Figure 7) shows a broad peak at about -400 mV vs SCE, due to the reduction of corrosion products, as shown by the thermodynamic potential $E_{th} = -128$ mV vs SCE [15] of the $\text{Cu}/\text{Cu}_2\text{O}$, H^+ equilibrium in the experimental conditions used. The strong anodic current in PEG solution in Figure 7 shows that the corrosion products dissolved. It is, in fact, quite common to find metallic compounds which are insoluble in water but which are soluble in polyethylene solution. This is the case with silver [16] and also with copper, giving the results in Figure 7. To conserve the patina it must be protected using an inhibitor here benzotriazole. In the presence of 10^{-3} mol l^{-1} of BTA, the current density of this cathodic peak increased to $-5 \mu\text{A cm}^{-2}$ as opposed to $-79 \mu\text{A cm}^{-2}$ for the solution without inhibitor. During anodic polarization, the plateau occurred only in the presence of benzotriazole. At $+200$ mV vs SCE, in

20% PEG 400 solution, the current density was $6.3 \mu\text{A cm}^{-2}$; when 10^{-3} M of BTA was added, it was limited to 1.6 nA cm^{-2} . Brostoff [17] has established that the complexes $\text{Cu(I)}/\text{BTA}$ and $\text{Cu(II)}/\text{BTA}$ can form at the surface of archaeological bronze in the presence of copper oxides, chlorides or carbonates. The reduction in anodic current density, as shown in Figure 7, demonstrates the effectiveness of BTA in H_2O -PEG solution on the copper corrosion products.

The impedance spectroscopy diagrams in Figure 8, obtained for copper covered with corrosion products, show an increase with BTA concentration: the diameter of the semicircle increases as the BTA concentration increases. The resistances R_p and R_{ad} increased with the amount of inhibitor (Table 1): the adsorption of BTA on the copper corrosion products and the formation of $\text{Cu(I)}/\text{BTA}$ and $\text{Cu(II)}/\text{BTA}$ complexes [17] ensured protection of the copper covered with its patina. The addition of a minimum concentration of 10^{-3} mol l^{-1} of benzotriazole ensured that the patina was preserved. In PEG solution with a concentration below 10^{-3} mol l^{-1} ,

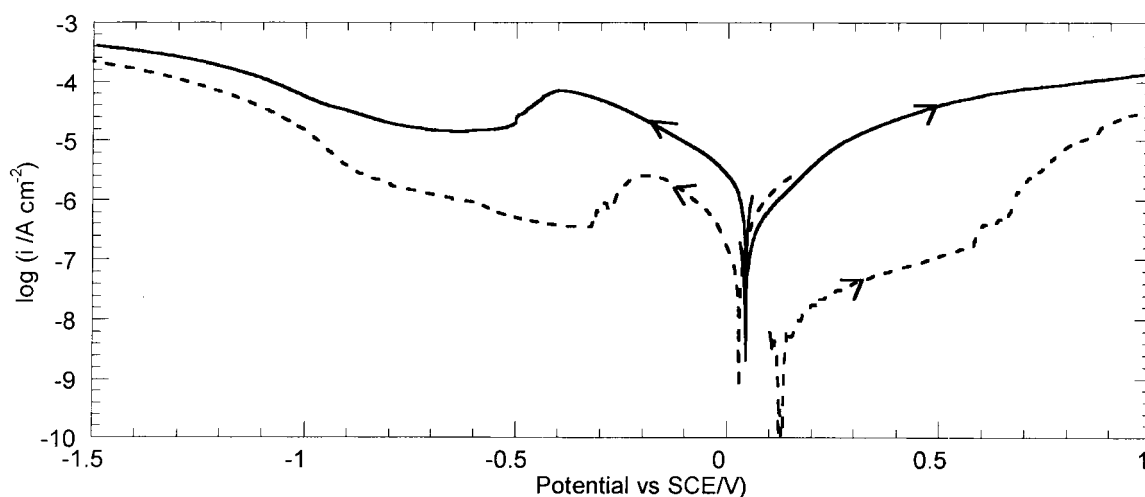


Fig. 7. Polarization curves of archaeological copper covered with corrosion products, at 25°C and 1 mV s^{-1} , in aqueous solutions of 20% PEG 400, with (---) and without (—) 10^{-3} mol l^{-1} of BTA.

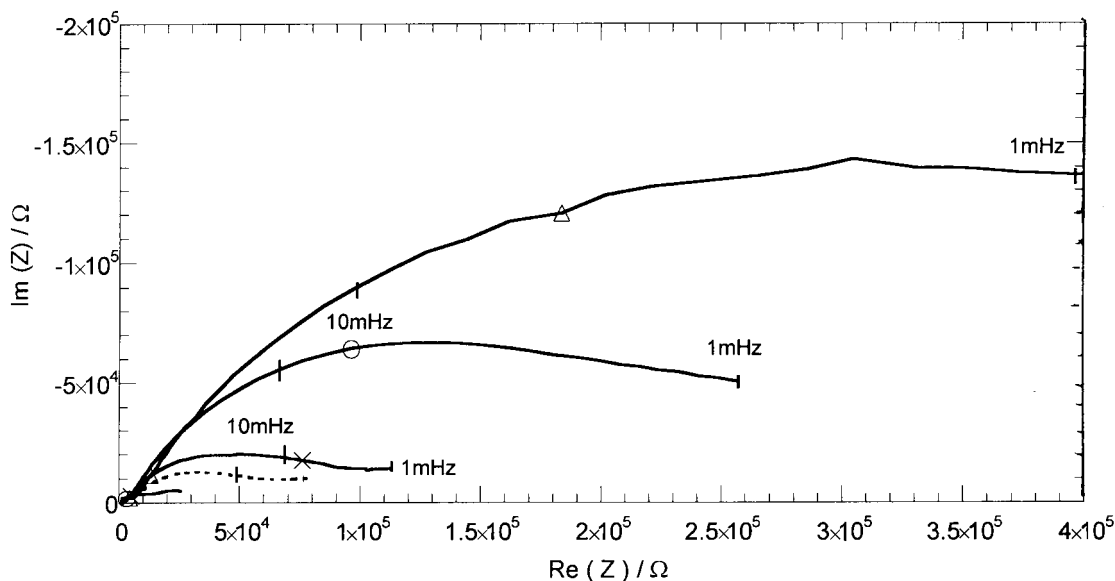


Fig. 8. Nyquist diagram showing impedance spectrum for archaeological copper covered with corrosion products, at corrosion potential, at 25 °C, in an aqueous solution of 20% PEG 400 with BTA. Amount of BTA: (—) 0, (- - -) 10^{-5} , (-x-) 10^{-3} , (-○-) 10^{-2} and (-△-) $8 \times 10^{-2} \text{ mol l}^{-1}$.

it was observed that the colour of the patina changed from green to brown, characteristic of dissolution of corrosion products.

3.3. Influence of immersion time

Impedance spectra were measured after different immersion times to check that the BTA was still efficient. Adsorption of PEG and BTA on the polished copper increased with time, since the diameter of the semicircle increased with time irrespective of the benzotriazole concentration (Figure 9). In the presence of corrosion

products, in a PEG 400 solution, the semicircle decreased with time (Figure 10), which corresponds to a reduction, over time, of the polarization resistance and, in particular, the adsorption resistance, in PEG solution. The dissolution current of the copper corrosion products thus increased with time. These results are in agreement with the degradation of the corrosion layer (change in color of the patina from green to brown). When $10^{-2} \text{ mol l}^{-1}$ of benzotriazole was added, the size of the capacitive loops increased with time (Figure 11), due essentially to the increase in adsorption resistance. Protection of the copper corrosion products by benzo-

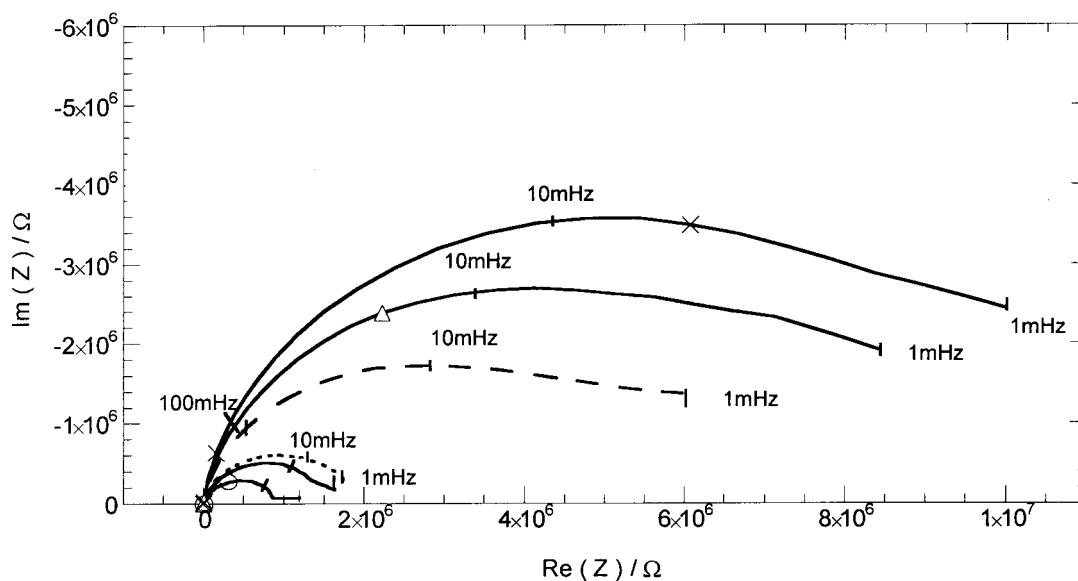


Fig. 9. Nyquist diagram showing impedance spectrum for polished copper, at corrosion potential, at 25 °C, in aqueous solution of 20% PEG 400 with or without $10^{-3} \text{ mol l}^{-1}$ of BTA, after different immersion times. Key: (-○-) PEG 4 h; (—) PEG 6 h; (- - -) PEG 8 h; (—) PEG + BTA 4 h; (-△-) PEG + BTA 6 h; (-x-) PEG + BTA 8 h.

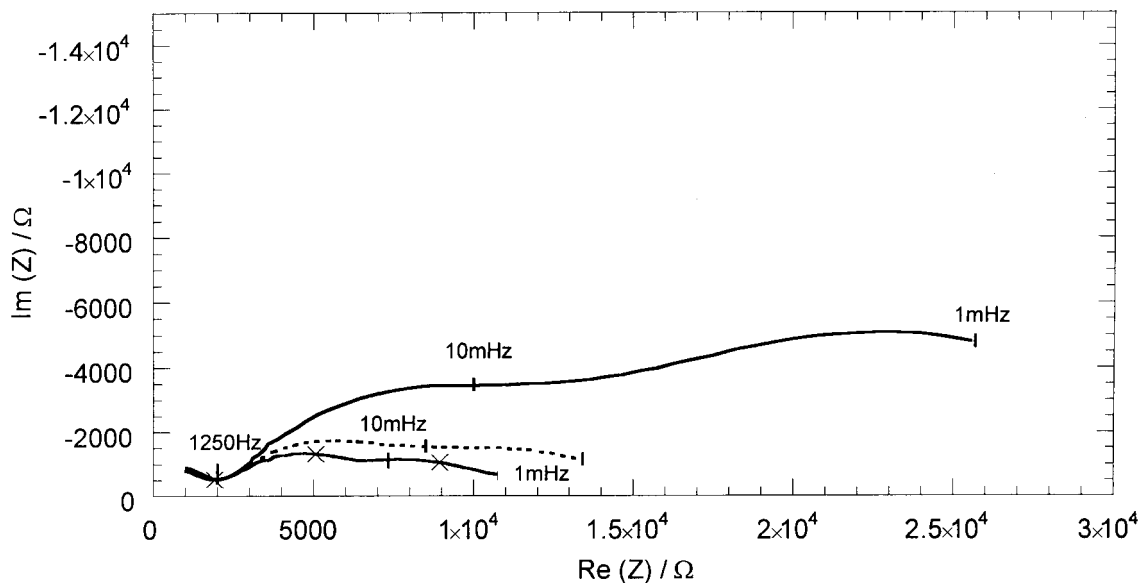


Fig. 10. Nyquist diagram showing impedance spectrum for archaeological copper covered with corrosion products, at corrosion potential, at 25 °C, in an aqueous solution of 20% PEG 400, after different immersion times. Key: (—) 10 h, (- - -) 12 h; (-×-) 14 h.

triazole thus increased with time. No change in the colour of the patina was observed in the presence of $10^{-2} \text{ mol l}^{-1}$ of BTA.

4. Conclusion

The polarization and impedance spectroscopy curves show the effectiveness of benzotriazole in H_2O -PEG 400 solution for both the polished copper and the covered copper. Through surface adsorption, polyethylene glycol protected polished copper by limiting its dissolution current. In this case, the use of a corrosion inhibitor is

not particularly justified. On the other hand, the anodic polarization curves and the impedance spectra revealed that the corrosion products dissolved in PEG 400 solution. When benzotriazole was added, the dissolution current of these corrosion products was significantly reduced. Protection of the corrosion layer of the copper was accentuated when the concentration of benzotriazole and the immersion time were increased. When corrosion products are present on archaeological copper, a corrosion inhibitor must be used during the wood impregnation phase. Benzotriazole, at a minimum concentration of $10^{-3} \text{ mol l}^{-1}$, is suitable for ensuring that the corrosion products are preserved.

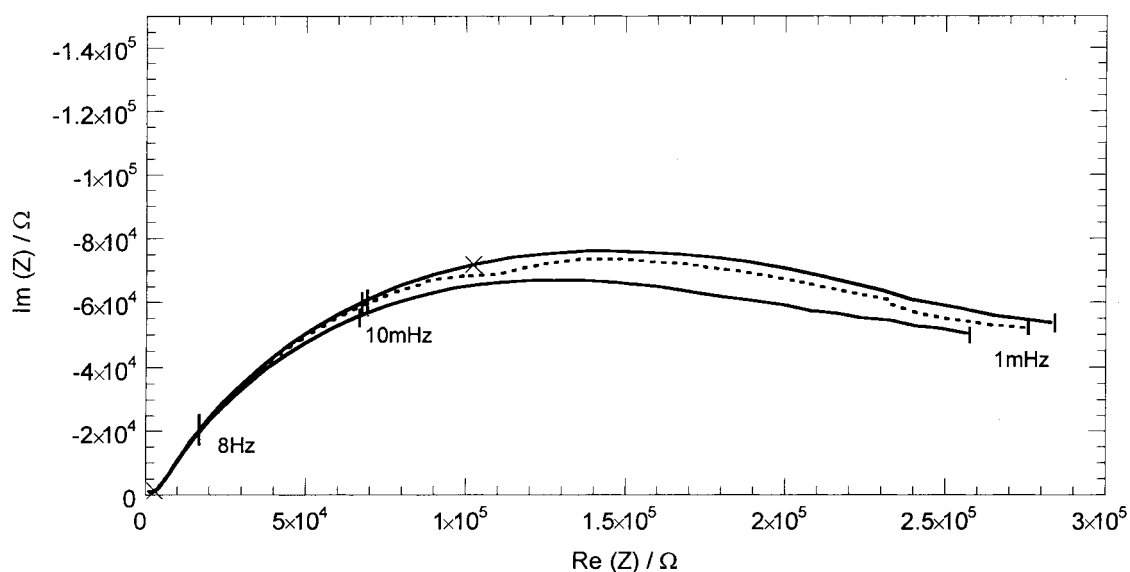


Fig. 11. Nyquist diagram showing impedance spectrum for archaeological copper covered with corrosion products, at corrosion potential, at 25 °C, in an aqueous solution of 20% PEG 400 with $10^{-2} \text{ mol l}^{-1}$ of BTA, after different immersion times. Key: (—) 10 h; (- - -) 12 h; (-×-) 14 h.

References

1. D. Grattan, *Studies in Conservation* **27** (1982) 124–136.
2. I.D. MacLeod, *Studies in Conservation* **36** (1991) 222–234.
3. L.S. Selwyn, D.A. Rennie-Bisaillon and N.E. Binnie, *Studies in Conservation* **38** (1993) 180–197.
4. V. Agyropoulos, J.J. Rameau, F. Dalard and C. Degrigny, Submitted to *Studies in Conservation*.
5. C. Clerc and R. Alkire, *J. Electrochem. Soc.* **138** (1991) 25–33.
6. P.G. Fox, G. Lewis and P.J. Boden, *Corros. Sci.* **19** (1979) 457–467.
7. E.A.A. Ashour, S.M. Sayed and B.G. Ateya, *J. Appl. Electrochem.* **25** (1995) 137–141.
8. J.D. Reid and A.P. David, *Plat. Surf. Finish.* **74** (1987) 66–70.
9. J.P. Diard, B. Le Gorrec and C. Montella, 'Cinétique Electrochimique', (Des Sciences et Des Arts, Hermann, Paris, 1996), pp. 85–97.
10. S. Kerit, F. Chaouket, A. Srihiri and M. Keddad, *J. Appl. Electrochem.* **24** (1994) 1139–45.
11. S.E. Faidi and J.D. Scantlebury, *J. Electrochem. Soc.* **136** (1989) 990–95.
12. A.M. Beccaria and C. Bertolotto, *Electrochim. Acta* **42** (1997) 1361–71.
13. E. Ahlberg and M. Friel, *Electrochim. Acta* **34** (1989) 1523–28.
14. Y.Z. Wang, A.M. Beccaria and G. Poggi, *Corros. Sci.* **36** (1994) 1277–88.
15. M. Pourbaix, 'Atlas d'Équilibres Electrochimiques' (Gauthier-Villars, Paris, 1963), p. 387.
16. A. Bouridah, 'Contribution à l'Étude des Propriétés de Transport Ionique d'Électrodes Polymères: les Polyéthers-sels de Lithium' Thèse de l'Institut National Polytechnique de Grenoble, France, June 1986.
17. L.B. Brostoff, 'Metal 95', James & James, 1997 pp. 99–108.